

**TECHNICAL EVALUATION OF THE HOLOGIC SELENIA
FULL FIELD DIGITAL MAMMOGRAPHY SYSTEM
WITH A TUNGSTEN TUBE**

**NHSBSP Equipment Report 0801
April 2008**

**K C Young and J M Oduko
National Coordinating Centre for the Physics of Mammography**

Enquiries

Enquiries about this report should be addressed to:

Professor KC Young

National Coordinating Centre for the Physics of Mammography

Medical Physics Department

Royal Surrey County Hospital

Guildford

GU2 7XX

Tel: 01483 406738

Fax: 01483 406742

Email: ken.young@nhs.net

Published by

NHS Cancer Screening Programmes

Fulwood House

Old Fulwood Road

Sheffield

S10 3TH

Tel: 0114 271 1060

Fax: 0114 271 1089

Email: info@cancerscreening.nhs.uk

Website: www.cancerscreening.nhs.uk

© NHS Cancer Screening Programmes 2008

The contents of this document may be copied for use by staff working in the public sector but may not be copied for any other purpose without prior permission from the NHS Cancer Screening Programmes.

The report is available in PDF format on the NHS Cancer Screening Programmes' website

Typeset by Prepress Projects Ltd, Perth (www.prepress-projects.co.uk)

Printed by Charlesworth

CONTENTS

	Page No
ACKNOWLEDGEMENTS	iv
1. INTRODUCTION	1
1.1 Testing procedures and performance standards for digital mammography	1
1.2 Objectives	1
2. METHODS	1
2.1 System tested	1
2.2 Detector response	1
2.3 Dose measurement	2
2.4 Contrast to noise ratio	2
2.5 Noise analysis	2
2.6 Image quality measurements	3
2.7 Optimisation	5
3. RESULTS	6
3.1 Detector response	6
3.2 AEC performance	7
3.3 Noise measurements	11
3.4 Image quality measurements	13
3.5 Comparison with other systems	13
3.6 Optimisation	20
4. DISCUSSION	22
5. CONCLUSIONS	23
REFERENCES	23

ACKNOWLEDGEMENTS

The authors are grateful to the staff at Hologic for their help in evaluating the unit at their factory.

1. INTRODUCTION

1.1 Testing procedures and performance standards for digital mammography

This report is one of a series evaluating commercially available digital mammography systems on behalf of the NHS Breast Screening Programme (NHSBSP). The testing methods and standards applied are mainly derived from NHSBSP Equipment Report 0604.¹ This is referred to in this document as the NHSBSP protocol and it has the same image quality and dose standards as those provided in the European protocol.^{2,3} The European protocol was followed where there is a more detailed performance standard, eg for the automatic exposure control (AEC) system.

1.2 Objectives

The purpose of these tests was to determine whether this system meets the main standards in the NHSBSP and European protocols and to provide performance data for comparison against other manufacturers' products. Additional measurements were also undertaken to assess how well the system's AEC was optimised. The method of assessing optimisation has been reported previously.^{4,5} Clinical evaluations are published separately by the NHSBSP where systems meet the minimum standards in the NHSBSP protocol. A final decision on the suitability of systems for use in the NHSBSP depends on a review of both the technical and clinical evaluations.

2. METHODS

2.1 System tested

The measurements were made on a new design of the Hologic Selenia digital mammography system which is fitted with an x-ray tube with a tungsten (W) target material. The tests were conducted at the Hologic factory in Danbury, Connecticut, USA. The system is equipped with a choice of either rhodium (Rh) or silver (Ag) filtration. The automatic exposure control (AEC) has three modes: standard dose, low dose and limited dose.

2.2 Detector response

The detector response was measured broadly as described in the NHSBSP protocol. A phantom of Plexiglas (PMMA) with a total thickness of 45 mm was positioned at the tube exit port and exposed using the two target/filter combinations available (W/Rh and W/Ag) at tube voltages spanning the range used clinically (25, 28, 31 and 34 kV). An ion chamber was positioned at the surface of the breast support table, and the entrance surface air kerma measured for a single tube current-time product for each tube voltage and target/filter combination tested. The readings were corrected to the surface of the imaging detector using the inverse square law. It was determined that the imaging detector is at a distance of 660 mm from the tube focus and 20 mm below the surface of the breast support table. No correction was made for attenuation by the protective plates above the detector but the grid was removed. The images were saved as unprocessed files and transferred to another computer for analysis. A 10 mm square region of interest (ROI) was positioned on the midline and 6 cm from

the chest wall edge of each image. The average pixel value and the standard deviation of pixel values within that region were measured. The relationship between average pixel values and the detector entrance surface air kerma was determined. The magnitude of the pixel offset at zero air kerma was determined.

2.3 Dose measurement

Doses were measured by using the AEC set to AUTOFILTER in each of its three dose modes to expose different thicknesses of PMMA. Small rigid expanded polystyrene spacers were added at the edge of the test object to adjust the total thickness to be equal to the equivalent breast thickness. Mean glandular doses (MGDs) were calculated for the equivalent breast thicknesses and the displayed doses recorded. To measure the contrast-to-noise ratio (CNR), an aluminium square, 10 × 10 mm and 0.2 mm thick, was placed on top of a 20 mm thick block, with one edge on the midline and 6 cm from the chest wall edge. Additional layers of PMMA were added on top to vary the total thickness.

2.4 Contrast to noise ratio

The images of the blocks of PMMA obtained during the dose measurement were analysed to obtain the CNRs. Twenty small, square ROIs (approximately 2.5 × 2.5 mm) were used to determine the average signal and the standard deviations in the signal within the image of the aluminium square (4 ROIs) and the surrounding background (16 ROIs). Small ROIs are used to minimise distortions due to the heel effect. However, this is less important for this system because flat-field correction is applied. The CNR was calculated for each image as defined in the NHSBSP and European protocols.

To apply the standards in the European protocol, the limiting value for CNR (using 50 mm PMMA) was determined according to equation 1. This equation determines the CNR value ($CNR_{limiting\ value}$) that is necessary to achieve the minimum threshold gold thickness for the 0.1 mm detail (ie $threshold\ gold_{limiting\ value} = 1.68\ \mu\text{m}$, which is equivalent to $threshold\ contrast_{limiting\ value} = 23.0\%$ using 28 kV Mo/Mo). Threshold contrasts were calculated as described in the European protocol and used in equation 1.

$$Threshold\ contrast_{measured} \cdot CNR_{measured} = Threshold\ contrast_{limiting\ value} \cdot CNR_{limiting\ value} \quad (1)$$

The relative CNR was then calculated according to equation 2 and compared with the limiting values provided for relative CNR shown in Table 1. The minimum CNR required to meet this criterion was then calculated.

$$Relative\ CNR = CNR_{measured} / CNR_{limiting\ value} \quad (2)$$

2.5 Noise analysis

The 45 mm thick block of PMMA with aluminium square used for the measurement of CNR was exposed using manually selected tube loading across the range available. The kV target/filter combination used was that selected by the AEC in standard dose mode. The compression paddle was in place. The same ROIs used in the CNR measurement were applied to the corresponding unprocessed images. The average standard deviations of the pixel values in the background ROI for each image were used to investigate the relationship between dose to the detector and image noise. It was assumed that this noise comprises three components – electronic noise, structural noise and quantum noise – with the relationship shown in equation 3. This method of analysis has been described previously.⁵

Table 1 Limiting values for relative CNR

Thickness of PMMA (mm)	Equivalent breast thickness (mm)	Limiting values for relative CNR (%) in European protocol
20	21	> 115
30	32	> 110
40	45	> 105
45	53	> 103
50	60	> 100
60	75	> 95
70	90	> 90

$$\sigma_p = \sqrt{k_e^2 + k_q^2 p + k_s^2 p^2} \quad (3)$$

where σ_p is the standard deviation in pixel values within an ROI with a uniform exposure and a mean pixel value p , and k_e , k_q and k_s are the coefficients determining the amount of electronic, quantum and structural noise in a pixel with a value p . For simplicity, the noise is generally presented here as relative noise defined as in equation 4.

$$\text{Relative noise} = \frac{\sigma_p}{p} \quad (4)$$

The variation in relative noise with mean pixel value was evaluated and fitted using equation 3, and non-linear regression was used to determine the best fit for the constants and their asymptotic confidence limits (using Graphpad Prism Version 4.03 for Windows, Graphpad software, San Diego, CA, USA; www.graphpad.com). This established whether the experimental measurements of the noise fitted this equation and the relative proportions of the different noise components. In fact the relationship between noise and pixel values has been found empirically to be approximated by a simple power relationship as shown in equation 5.

$$\frac{\sigma_p}{p} = k_t p^{-n} \quad (5)$$

where k_t is a constant. If the noise were purely quantum noise the value of n would be 0.5. However, the presence of electronic and structural noise means that n can be slightly higher or lower than 0.5.

2.6 Image quality measurements

Contrast detail measurements were made using the CDMAM phantom (version 3.4, UMC St. Radboud, Nijmegen University, Netherlands). The phantom was positioned with a 20 mm thickness of PMMA above and below, to give a total attenuation approximately equivalent to 50 mm of PMMA or 60 mm thickness of typical breast tissue. This arrangement was imaged using the x-ray set's AEC in standard dose mode with small rigid expanded polystyrene spacers in place to create a total thickness of 60 mm. This procedure was repeated with small adjustments to the phantom position to obtain a representative sample of 16 images at this dose level. Unprocessed images were transferred to disk for subsequent analysis off-site. Further images of the test phantom were then obtained at other dose levels by manually selecting higher and lower mAs values with the same beam quality as selected under AEC control.

Technical Evaluation of the Hologic Selenia FFDM System with a Tungsten Tube

An automatic method of reading the CDMAM images was used.^{6,7} The threshold gold thickness for a typical human observer was predicted using equation 6.

$$TC_{predicted} = r TC_{auto} \quad (6)$$

where $TC_{predicted}$ is the predicted threshold contrast for a typical observer and TC_{auto} is the threshold contrast measured using an automated procedure with CDMAM images. Contrasts were calculated from gold thickness for a nominal tube voltage of 28 kV and a Mo/Mo target/filter combination as described in the European protocol. r is the average ratio between human and automatic threshold contrast determined experimentally with the values shown in Table 2.⁶

The main advantage of automatic reading is that it has the potential of eliminating observer error, which is a significant problem when using human observers. However, it should be noted that at the present time the official protocols are based on human reading.

The predicted threshold gold thickness for each detail diameter at each dose level was fitted with a curve as described in the NHSBSP protocol. The confidence limits for the predicted threshold gold thicknesses have been previously determined by a resampling method using a large set of images. The threshold contrasts quoted in the tables of results are derived from the fitted curves, as this has been found to improve the accuracy.⁶

The expected relationship between threshold contrast and dose is shown in equation 7.

Table 2 Values of r used to predict threshold contrast

Diameter of gold disc (mm)	Average ratio of human to automatically measured threshold contrast (r)
0.08	1.40
0.10	1.50
0.13	1.60
0.16	1.68
0.20	1.75
0.25	1.82
0.31	1.88
0.40	1.94
0.50	1.98
0.63	2.01
0.80	2.06
1.00	2.11

$$\text{Threshold contrast} = \lambda D^{-n} \quad (7)$$

D represents the MGD for a 60 mm thick standard breast equivalent to the test phantom configuration used for the image quality measurement. λ is a constant to be fitted. It is assumed that a similar equation applies when using threshold gold thickness instead of contrast. This equation was plotted with the experimental data for the 0.1 and 0.25 mm details. The appropriate value of n was determined from the analysis of the noise as a function of the pixel value. In practice, this was done by finding the value of n that provided the best fit to the experimental data.

2.7 Optimisation

A method for determining optimal beam qualities and exposure factors for digital mammography systems has been described previously and was used to evaluate this system.^{4,5} CNR and mean glandular dose were measured as described above using blocks of PMMA from 20 to 70 mm thick. For each thickness, four tube voltage settings were used (25, 28, 31 and 34 kV) with each of the target/filter combinations available (W/Rh and W/Ag) and the mAs recorded. The MGDs to typical breasts with attenuation equivalent to each thickness of the PMMA were calculated as described in the NHSBSP protocol. Each exposure was designed to achieve a standard pixel value by using the AEC in automatic mAs mode. Additional CNR measurements were made with a 45 mm thickness of PMMA using the AEC selected beam quality and a wide range of manually selected mAs values. The relationship between noise and pixel values in digital mammography systems has been previously⁵ shown to be approximated by

$$\text{Relative noise} = \frac{\sqrt{\frac{sd(bgd)^2 + sd(Al)^2}{2}}}{p} = k_i p^{-n} \quad (8)$$

where k_i is a constant and p is the average background pixel value linearised with absorbed dose to the detector. $sd(bgd)$ is the average standard deviation of pixel values in the ROIs over the background. $sd(Al)$ is the average standard deviation of pixel values in an ROI over a $0.2 \times 10 \times 10$ mm piece of aluminium. The value of n was found by fitting this equation to the experimental data. Equation 9 was then used to calculate the dose required to achieve a target CNR, where k is a constant to be fitted and D is the MGD for a breast of equivalent thickness.

$$\text{CNR} = kD^n \quad (9)$$

The target CNR was that calculated to reach either the minimum or achievable image quality in the NHSBSP and European protocols using the following relationship.

$$\text{Threshold contrast} = \frac{\lambda}{\text{CNR}} \quad (10)$$

where λ is a constant that is independent of dose, beam quality and the thickness of attenuating material. The optimal beam quality for each thickness was selected as that necessary to achieve the target CNR for the minimum dose.

3. RESULTS

3.1 Detector response

The detector was found to have a linear response with a pixel value offset of 39, as shown in Figure 1. The manufacturer indicates that an offset of 50 is set for the detector response. The gradient was measured to be 0.196 μGy per pixel value at 28 kV W/Rh. The exposures selected by the AEC resulted in average pixel values in the range of 200–600 depending on the mode selected, and after deducting the offset. A standard value of 500 was chosen to determine the reference entrance air kerma, which was 90.3 μGy using 28 kV W/Rh. In practice, attenuation by protective plates will make the true value somewhat lower than this. The corresponding reference entrance air kermas to produce pixel values of 500 using other beam qualities are shown in Figure 2.

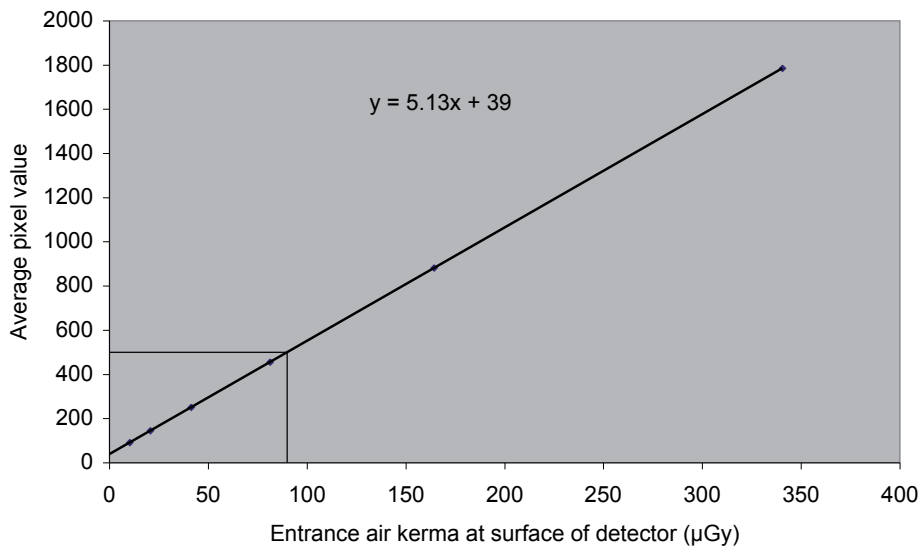


Figure 1 Detector response.

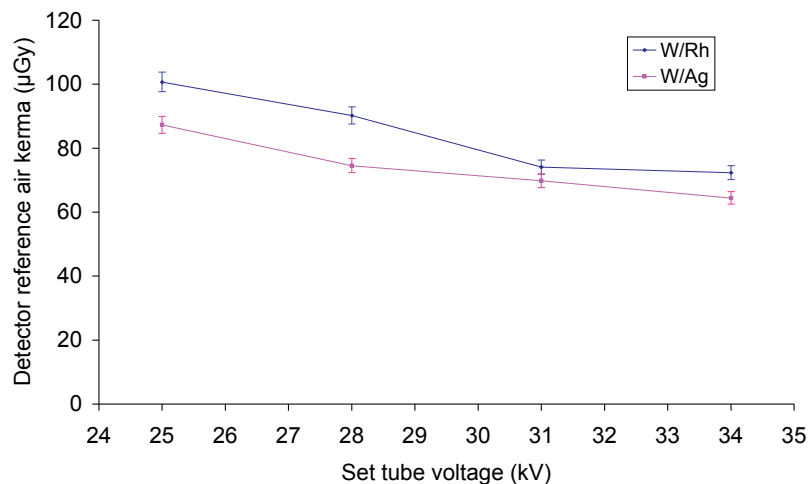


Figure 2 Detector reference air kerma for a pixel value of 500 after removing offset of 50.

3.2 AEC performance

3.2.1 Dose

The MGDs for breasts simulated with PMMA exposed under AEC control are shown in Table 3 and Figure 3 for the three AEC modes available. At all thicknesses the dose was below the remedial level in the NHSBSP protocol, which is the same as the maximum acceptable level in the European protocol.

3.2.2 CNR

The results of the contrast and CNR measurements are shown in Table 4 and Figure 4. The CNR required to meet the minimum acceptable and achievable image quality (IQ) standards at the 60 mm breast thickness have been calculated and are shown in Table 4 and Figure 4. The CNR required at each thickness to meet the limiting values for CNR in the European protocol is also shown.

Table 3a Mean glandular dose for simulated breasts (AEC in standard dose mode)

PMMA thickness (mm)	Equivalent breast thickness (mm)	kV	Target	Filter	mAs	MGD (mGy) ^a	Displayed dose (mGy)	NHSBSP remedial level (mGy)
20	21	25	W	Rh	40.9	0.60	0.56	>1.0
30	32	26	W	Rh	61.9	0.82	0.75	>1.5
40	45	28	W	Rh	83.3	1.17	1.03	>2.0
45	53	28	W	Rh	113.0	1.47	1.24	>2.5
50	60	30	W	Rh	106.7	1.58	1.33	>3.0
60	75	29	W	Ag	125.9	2.00	1.58	>4.5
70	90	32	W	Ag	132.8	2.50	2.03	>6.5
80	103	35	W	Ag	111.6		2.32	

^aThe dose calculation software does not include simulations with thicknesses of PMMA greater than 70 mm.

Table 3b Mean glandular dose for simulated breasts (AEC in low dose mode)

PMMA thickness (mm)	Equivalent breast thickness (mm)	kV	Target	Filter	mAs	MGD (mGy)	Displayed dose (mGy)	NHSBSP remedial level (mGy)
20	21	25	W	Rh	30.0	0.44	0.40	>1.0
30	32	26	W	Rh	45.9	0.61	0.56	>1.5
40	45	28	W	Rh	60.4	0.85	0.75	>2.0
45	53	28	W	Rh	82.0	1.08	0.90	>2.5
50	60	29	W	Rh	92.2	1.24	1.03	>3.0
60	75	27	W	Ag	133.0	1.56	1.25	>4.5
70	90	31	W	Ag	113.0	1.97	1.56	>6.5
80	103	34	W	Ag	96.3		1.85	

Technical Evaluation of the Hologic Selenia FFDM System with a Tungsten Tube

Table 3c Mean glandular dose for simulated breasts (AEC in limited dose mode)

PMMA thickness (mm)	Equivalent breast thickness (mm)	kV	Target	Filter	mAs	MGD (mGy)	Displayed dose (mGy)	NHSBSP remedial level (mGy)
20	21	25	W	Rh	18.5	0.27	0.25	>1.0
30	32	26	W	Rh	25.8	0.34	0.31	>1.5
40	45	28	W	Rh	33.7	0.48	0.42	>2.0
45	53	28	W	Rh	49.9	0.65	0.55	>2.5
50	60	29	W	Rh	55.9	0.75	0.63	>3.0
60	75	30	W	Rh	86.6	1.14	0.92	>4.5
70	90	28	W	Ag	101.6	1.23	0.97	>6.5
80	103	31	W	Ag	93.1		1.35	

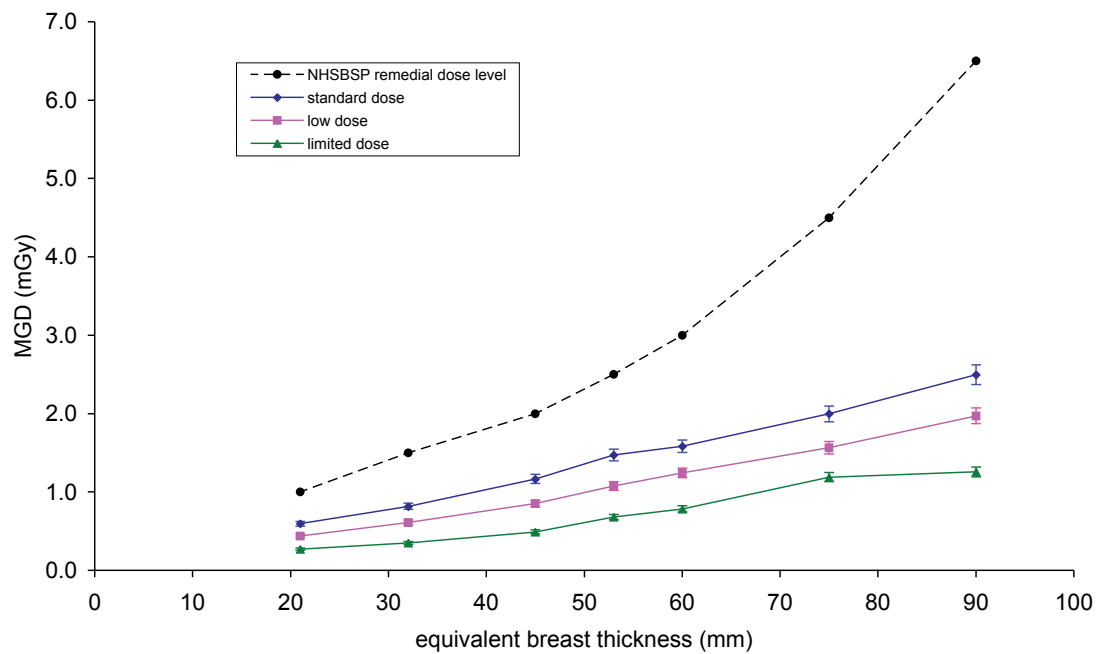


Figure 3 MGD for different thicknesses of simulated breasts using the three AEC modes.

Technical Evaluation of the Hologic Selenia FFDM System with a Tungsten Tube

Table 4a Contrast and CNR measurements (AEC in standard dose mode)

Equivalent breast thickness (mm)	kV target/ filter	mAs	Back-ground pixel value ^a	% contrast for 0.2 mm Al	Measured CNR	CNR at minimum acceptable IQ	CNR at achievable IQ	CNR to meet European limiting value	European limiting values for relative CNR
21	25 W/Rh	40.9	535	18.0	10.58	4.14	6.03	4.76	>115
32	26 W/Rh	61.9	531	16.8	9.61	4.14	6.03	4.56	>110
45	28 W/Rh	83.3	530	15.6	8.70	4.14	6.03	4.35	>105
53	28 W/Rh	113.0	535	15.2	8.59	4.14	6.03	4.27	>103
60	30 W/Rh	106.7	503	14.3	7.51	4.14	6.03	4.14	>100
75	29 W/Ag	125.9	582	12.3	6.87	4.14	6.03	3.94	>95
90	32 W/Ag	132.8	609	10.9	6.03	4.14	6.03	3.73	>90
103	35 W/Ag	111.6	533	9.1	4.43	4.14	6.03		

^aBackground pixel values after subtracting an offset of 50.

Table 4b Contrast and CNR measurements (AEC in low dose mode)

Equivalent breast thickness (mm)	kV target/ filter	mAs	Back-ground pixel value ^a	% contrast for 0.2 mm Al	Measured CNR	CNR at minimum acceptable IQ	CNR at achievable IQ	CNR to meet European limiting value	European limiting values for relative CNR
21	25 W/Rh	30.0	366	18.1	8.51	4.14	6.03	4.76	>115
32	26 W/Rh	45.9	381	16.9	7.98	4.14	6.03	4.56	>110
45	28 W/Rh	60.4	379	15.7	7.36	4.14	6.03	4.35	>105
53	28 W/Rh	82.0	370	15.4	7.02	4.14	6.03	4.27	>103
60	29 W/Rh	92.2	362	14.8	6.61	4.14	6.03	4.14	>100
75	27 W/Ag	133.0	413	13.4	6.24	4.14	6.03	3.94	>95
90	31 W/Ag	113.0	435	11.8	5.43	4.14	6.03	3.73	>90
103	34 W/Ag	96.3	382	10.2	4.17	4.14	6.03		

^aBackground pixel values after subtracting an offset of 50.

Technical Evaluation of the Hologic Selenia FFDM System with a Tungsten Tube

Table 4c Contrast and CNR measurements (AEC in limited dose mode)

Equivalent breast thickness (mm)	kV target/filter	mAs	Back-ground pixel value ^a	% contrast for 0.2 mm Al	Measured CNR	CNR at minimum acceptable IQ	CNR at achievable IQ	CNR to meet European limiting value	European limiting values for relative CNR
21	25 W/Rh	18.5	205	18.4	5.73	4.14	6.03	4.76	>115
32	26 W/Rh	25.8	194	17.4	5.21	4.14	6.03	4.56	>110
45	28 W/Rh	33.7	195	16.1	4.80	4.14	6.03	4.35	>105
53	28 W/Rh	49.9	201	15.7	4.73	4.14	6.03	4.27	>103
60	29 W/Rh	55.9	200	15.1	4.52	4.14	6.03	4.14	>100
75	30 W/Rh	86.6	223	14.2	4.51	4.14	6.03	3.94	>95
90	28, W/Ag	101.6	222	13.0	4.04	4.14	6.03	3.73	>90
103	31, W/Ag	93.1	211	11.7	3.44	4.14	6.03		

^aBackground pixel values after subtracting an offset of 50.

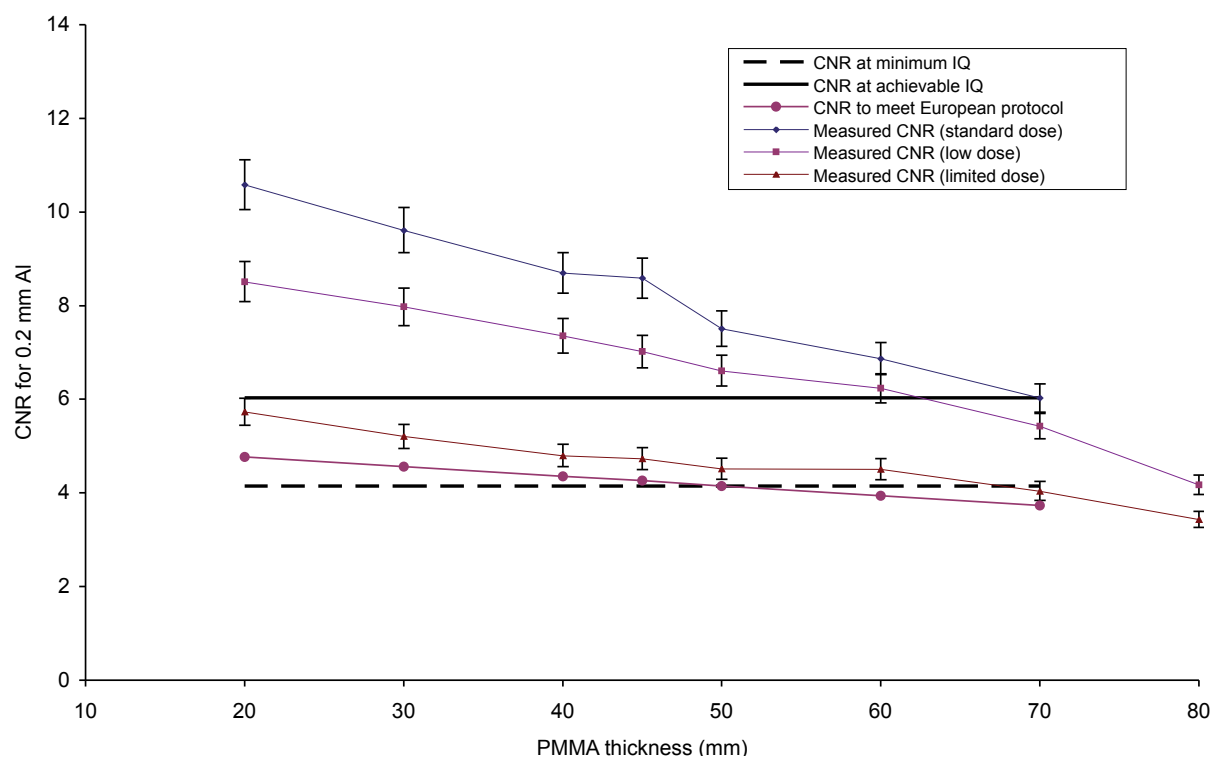


Figure 4 Measured CNR compared with the limiting values in the European protocol for the system. Error bars indicate 95% confidence limits.

3.3 Noise measurements

The variation in noise with dose was analysed by plotting the standard deviation in pixel values against the detector entrance air kerma, as shown in Figure 5. The fitted power curve has an index of 0.356. If only quantum noise sources were present, the data would form a straight line with an index of 0.5. The presence of some electronic noise and structural noise has caused the curve to deviate from a straight line. This is normal for such systems, and quantum noise was the dominant noise source.

The relative noise is plotted against the background pixel value (after removing the offset) in Figure 6. The offset corrected pixel value is proportional to the dose absorbed by the detector. A curve of the form described in equation 5 with an index $n = 0.65$ has been fitted to the measured data. A value of n of 0.5 would be expected if only quantum noise were present.

Figure 7 is an alternative way of presenting the data and shows the relative noise at different average pixel values. The estimated relative contributions of electronic, structural and quantum noise are shown and the quadratic sum of these contributions fitted to the measured noise using equation 3.

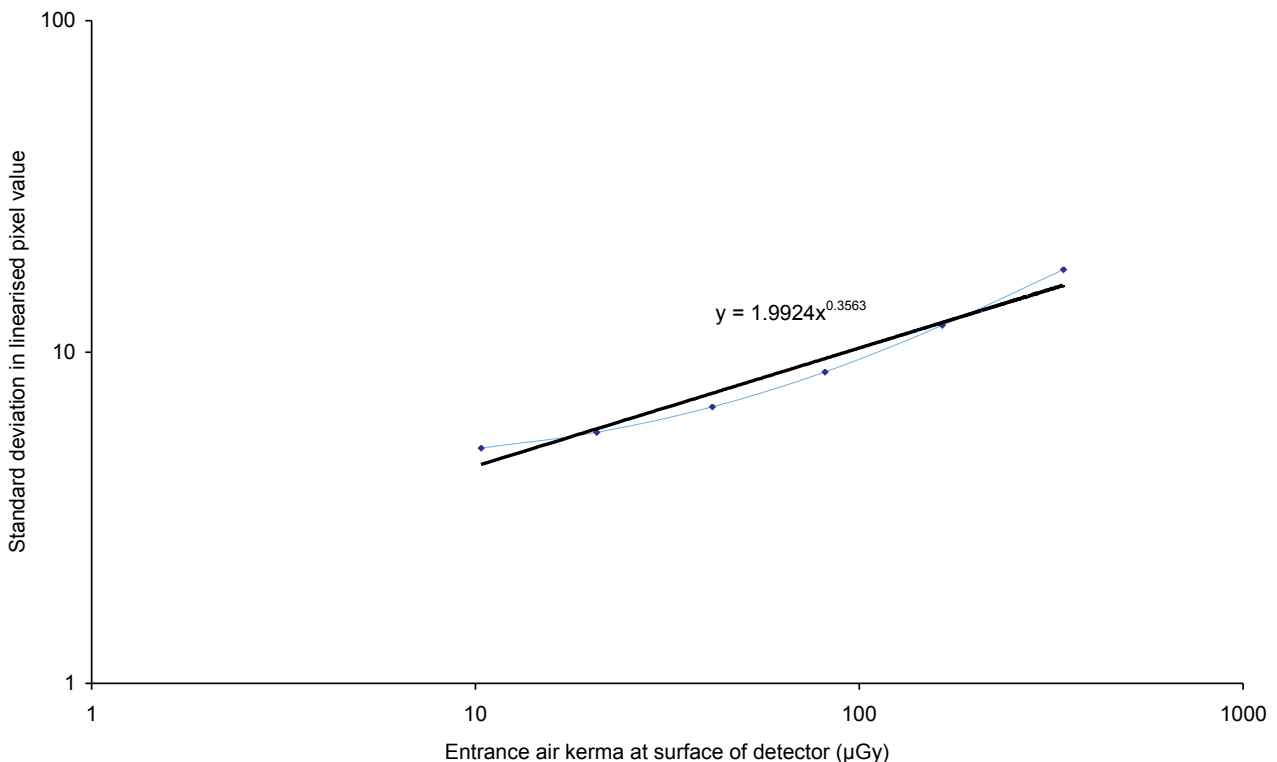


Figure 5 Standard deviation of pixel values versus air kerma at detector.

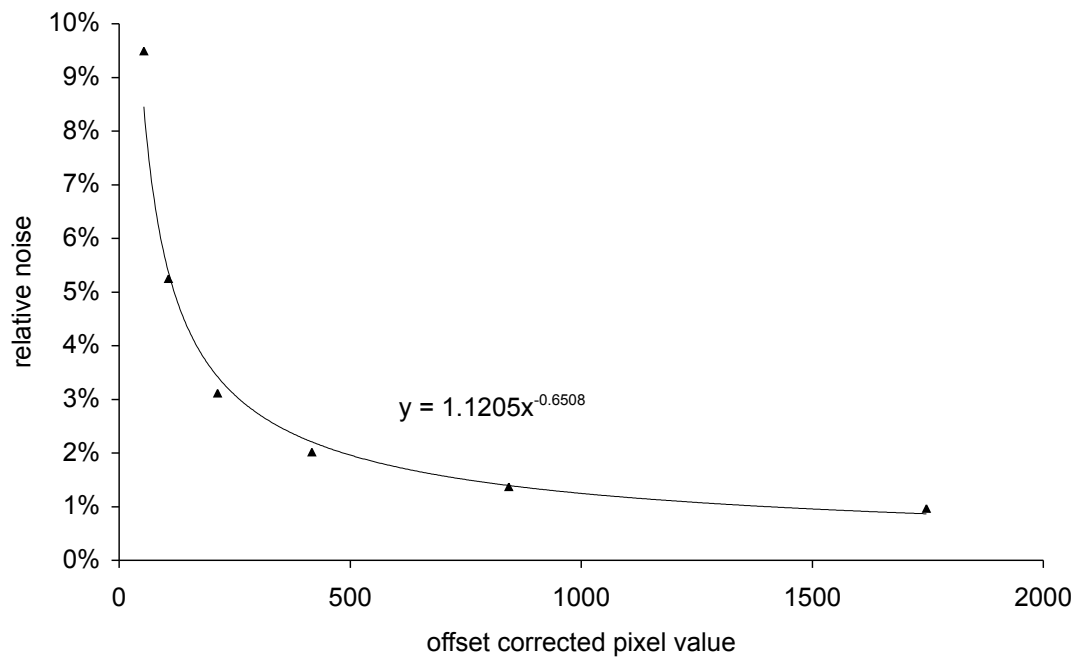


Figure 6 Relative noise at different pixel values.

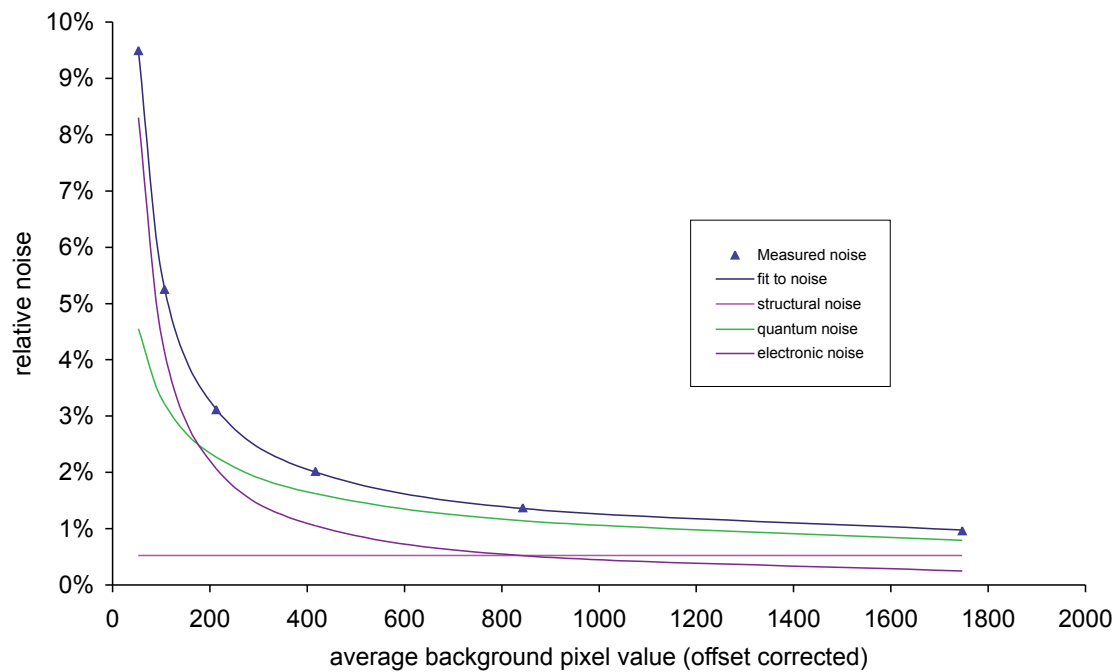


Figure 7 Relative noise and noise components at different pixel values.

3.4 Image quality measurements

The first exposures of the image quality phantom were made using the AEC in standard dose mode to select the beam quality and exposure factors. This resulted in the selection of 30 kV W/Rh and 109 mAs and an MGD of 1.68 mGy to an equivalent breast (60 mm thick). Subsequent image quality measurements were made at approximately quarter, half, double and treble this dose by manual selection of the mAs at the same beam quality, as shown in Table 5.

The contrast detail curves at the five dose levels are shown in Figure 8. The threshold gold thicknesses for different diameters and the five different dose levels for this system are shown in Table 6, along with the minimum and achievable threshold values from the NHSBSP protocol (ie same as the European protocol). The data in Table 6 are taken from the fitted curves rather than the raw data.

The measured threshold gold thicknesses are plotted against the MGD for an equivalent breast for the 0.1 and 0.25 mm detail sizes in Figure 9. This shows how the threshold gold thickness reduced as the dose was increased. The fitted curves in Figure 9 were used to determine the doses required to meet the minimum acceptable and achievable image quality levels for comparison with other systems in the next section. The fitted curves such as shown in Figure 9 were used to determine the doses required to meet the minimum acceptable and achievable image quality levels for detail sizes from 0.1 to 1.0 mm and are shown in Figure 10.

3.5 Comparison with other systems

The MGDs to reach the minimum and achievable image quality standards in the NHSBSP protocol have been estimated from the curves shown in Figure 9. (The error in estimating these doses depends on the accuracy of the curve fitting procedure, and pooled data for several systems have been used here to estimate 95% confidence limits of about 20%.) These doses are shown against similar data for other models of digital mammography system in Tables 7 and 8 and Figures 11 to 14. The data for the other systems have been determined in the same way as described in this report and the results published previously.⁸⁻¹² The data for film-screens represent an average value determined using a variety of modern film-screen systems.

Table 5 Images acquired for image quality measurement

Exposure mode	kV target/filter	Tube loading (mAs)	Mean glandular dose to equivalent breasts 60 mm thick (mGy)	Number of CDMAM images acquired and analysed
Manual	30 W/Rh	27.4	0.42	8
Manual	30 W/Rh	54.8	0.85	16
AEC (standard dose)	30 W/Rh	108.9	1.68	16
Manual	30 W/Rh	219.7	3.39	16
Manual	30 W/Rh	348.2	5.37	8

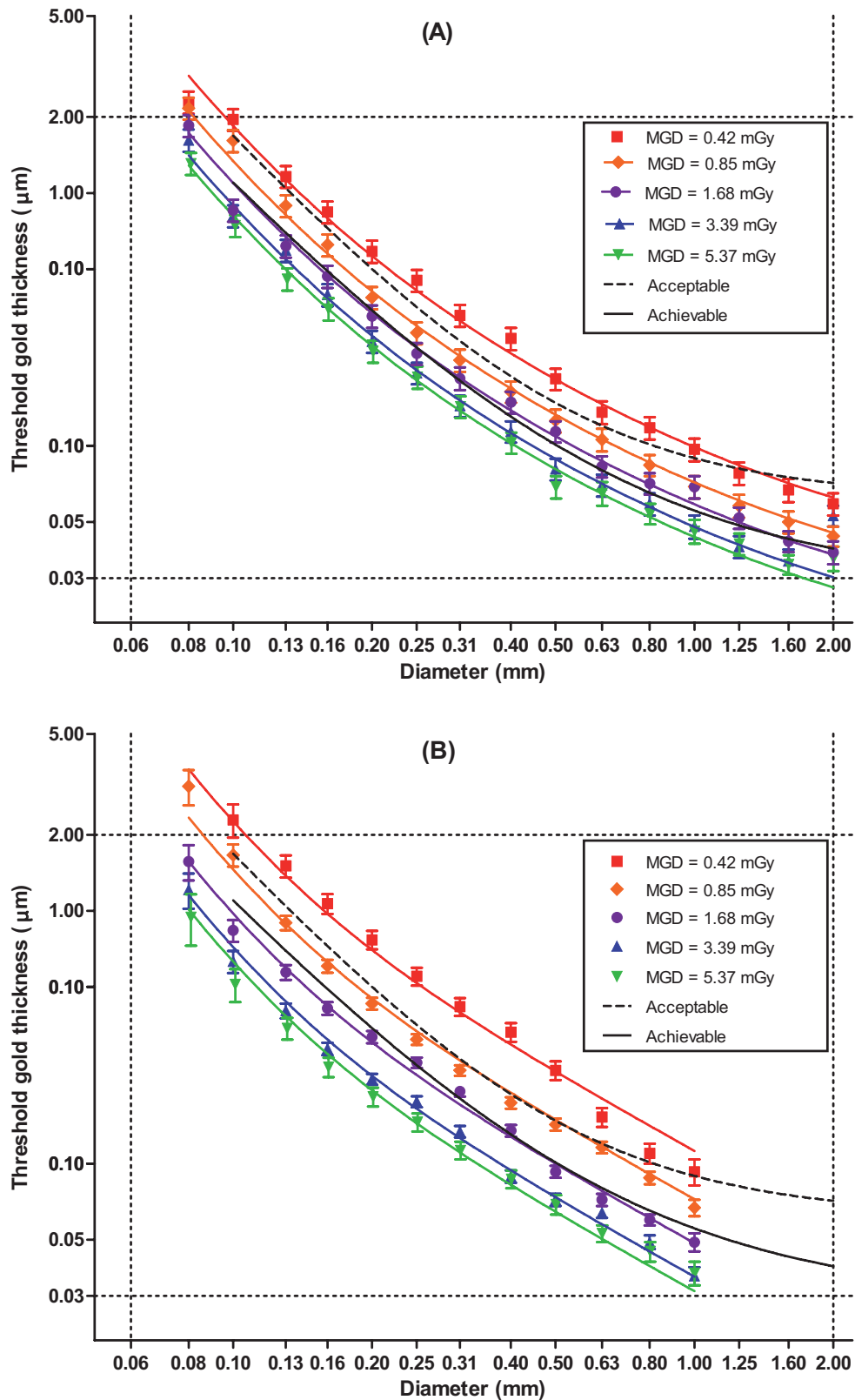


Figure 8 Contrast-detail curves for the system for five different doses at 30kV W/Rh using (a) human readers and (b) predicted results from automated reading. The 1.68 mGy dose corresponds to the AEC selection in standard dose mode. Error bars indicate 95% confidence limits.

Technical Evaluation of the Hologic Selenia FFDM System with a Tungsten Tube

Table 6a Average threshold gold thicknesses for different detail diameters for five different doses using 30kV W/Rh (human readers)

Diameter (mm)	Threshold gold thickness (μm)						
	Acceptable value	Achievable value	MGD = 0.42 mGy	MGD = 0.85 mGy	MGD = 1.68 mGy (AEC standard dose)	MGD = 3.39 mGy	MGD = 5.37 mGy
0.1	1.680	1.100	1.82 \pm 0.182	1.559 \pm 0.156	1.065 \pm 0.106	1.001 \pm 0.10	0.874 \pm 0.087
0.25	0.352	0.244	0.450 \pm 0.045	0.294 \pm 0.029	0.241 \pm 0.024	0.196 \pm 0.02	0.174 \pm 0.017
0.5	0.150	0.103	0.193 \pm 0.019	0.130 \pm 0.013	0.114 \pm 0.011	0.085 \pm 0.008	0.080 \pm 0.008
1	0.091	0.056	0.093 \pm 0.009	0.069 \pm 0.007	0.061 \pm 0.006	0.050 \pm 0.005	0.047 \pm 0.005

Table 6b Average threshold gold thicknesses for different detail diameters for five different doses using 30kV W/Rh (automatically predicted data)

Diameter (mm)	Threshold gold thickness (μm)						
	Acceptable value	Achievable value	MGD = 0.42 mGy	MGD = 0.85 mGy	MGD = 1.68 mGy (AEC standard dose)	MGD = 3.39 mGy	MGD = 5.37 mGy
0.1	1.680	1.100	2.338 \pm 0.234	1.596 \pm 0.16	0.865 \pm 0.087	0.61 \pm 0.061	0.504 \pm 0.051
0.25	0.352	0.244	0.558 \pm 0.027	0.311 \pm 0.015	0.233 \pm 0.011	0.166 \pm 0.008	0.143 \pm 0.007
0.5	0.150	0.103	0.213 \pm 0.012	0.137 \pm 0.007	0.099 \pm 0.005	0.074 \pm 0.004	0.068 \pm 0.004
1	0.091	0.056	0.095 \pm 0.007	0.073 \pm 0.005	0.049 \pm 0.004	0.039 \pm 0.003	0.037 \pm 0.003

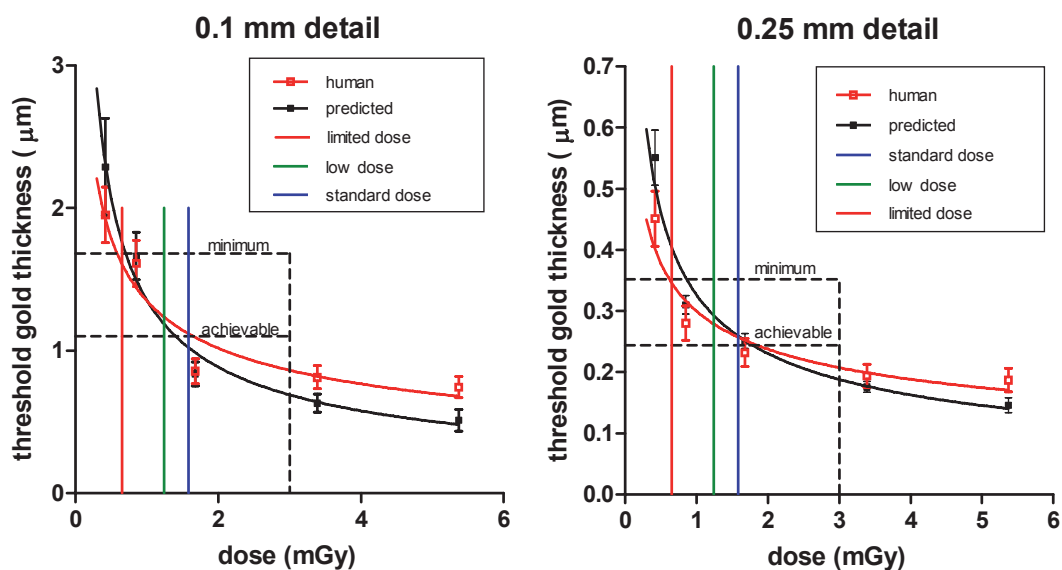


Figure 9 Threshold gold thickness at different doses for human and predicted reading. Error bars indicate 95% confidence limits. The doses selected for a 5 cm thickness of PMMA using the three AEC dose modes are shown by the coloured vertical lines.

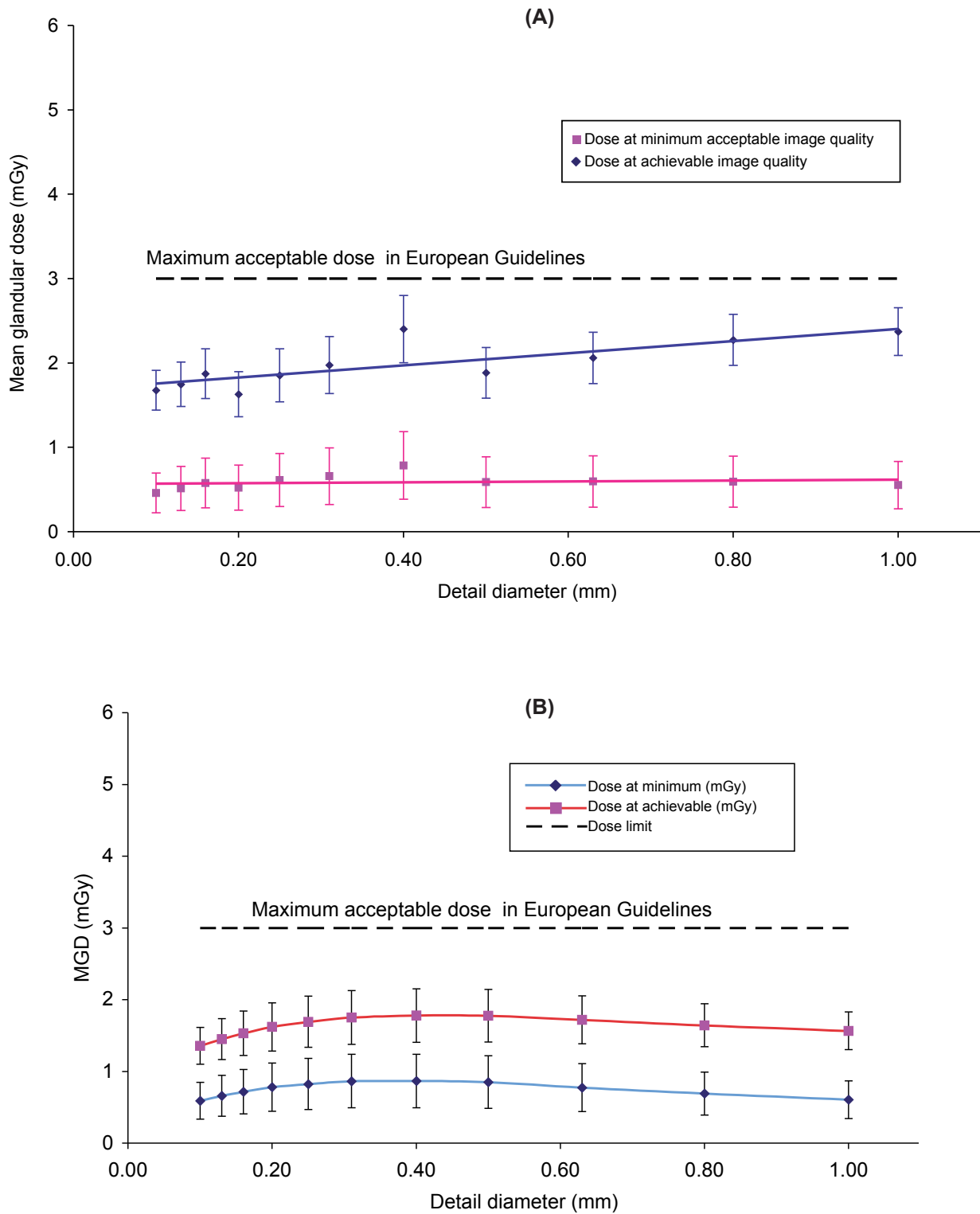


Figure 10 The MGD calculated to be necessary to reach the achievable and minimum acceptable image quality levels at different detail sizes using 30 kV W/Rh for an equivalent breast 60 mm thick: (a) human readings, (b) predicted readings.

Technical Evaluation of the Hologic Selenia FFDM System with a Tungsten Tube

Table 7 The MGD for different systems to reach the minimum threshold gold thickness for 0.1 and 0.25 mm details

System	MGD (mGy) for 0.1 mm		MGD (mGy) for 0.25 mm	
	Human	Predicted	Human	Predicted
Fischer Senovision	0.55	0.42	0.48	0.53
Sectra MDM	0.60	0.82	0.67	0.46
Siemens Novation ^a	0.63	0.61	0.52	0.63
Siemens Novation ^b	0.44	0.56	0.41	0.71
Hologic Selenia (Mo)	0.85	0.55	0.80	0.53
Hologic Selenia (W)	0.58	0.71	0.65	0.64
GE DS	1.01	0.82	0.87	0.83
Film-screen	1.17	1.30	1.07	1.36
Fuji Profect CR	1.67	1.78	1.45	1.35
Agfa CR 85-X	2.00	1.94	0.86	1.42
Kodak CR (EHR-M2)	2.29	2.34	1.45	1.80
Kodak CR (EHR-M)	3.46	2.49	1.49	1.33
Test CR	4.52	4.17	2.33	2.12

^aSystem at Erlangen.

^bSystem at Cambridge.

Table 8 The MGD for different systems to reach the achievable threshold gold thickness for 0.1 and 0.25 mm details

System	MGD (mGy) for 0.1 mm		MGD (mGy) for 0.25 mm	
	Human	Predicted	Human	Predicted
Fischer Senovision	1.16	0.90	0.98	1.09
Sectra MDM	1.27	1.74	1.37	0.95
Siemens Novation ^a	1.56	1.21	1.14	1.27
Siemens Novation ^b	1.03	1.30	0.85	1.47
Hologic Selenia (Mo)	1.84	1.19	1.68	1.12
Hologic Selenia (W)	1.66	1.37	1.61	1.48
GE DS	2.35	1.57	1.80	1.87
Film-screen	2.48	3.03	2.19	2.83
Fuji Profect CR	4.26	3.29	3.52	2.65
Agfa CR 85-X	5.03	4.88	2.20	3.15
Kodak CR (EHR-M2)	5.34	5.45	3.03	3.74
Kodak CR (EHR-M)	7.74	5.56	6.28	5.60
Test CR	11.5	9.90	5.96	5.63

^aSystem at Erlangen.

^bSystem at Cambridge.

Technical Evaluation of the Hologic Selenia FFDM System with a Tungsten Tube

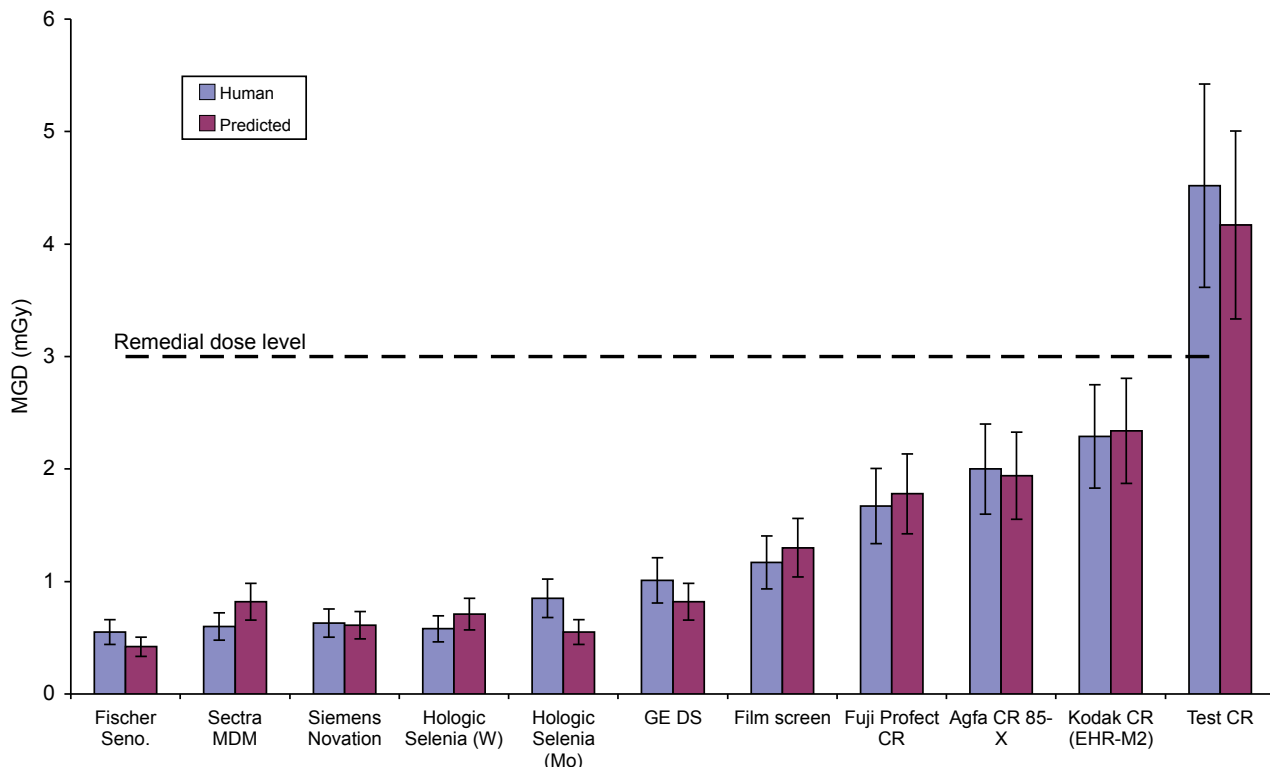


Figure 11 Dose to reach minimum acceptable image quality standard for 0.1 mm detail. Error bars indicate 95% confidence limits.

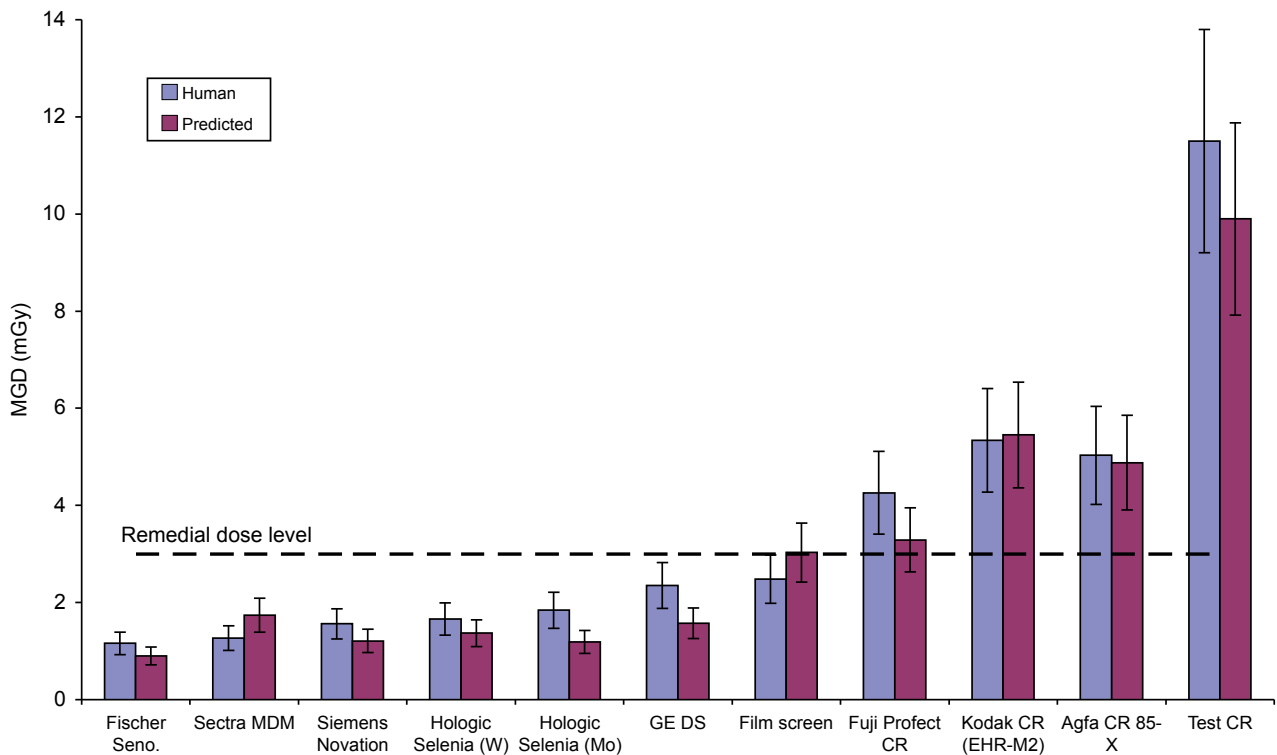


Figure 12 Dose to reach achievable image quality standard for 0.1 mm detail. Error bars indicate 95% confidence limits.

Technical Evaluation of the Hologic Selenia FFDM System with a Tungsten Tube

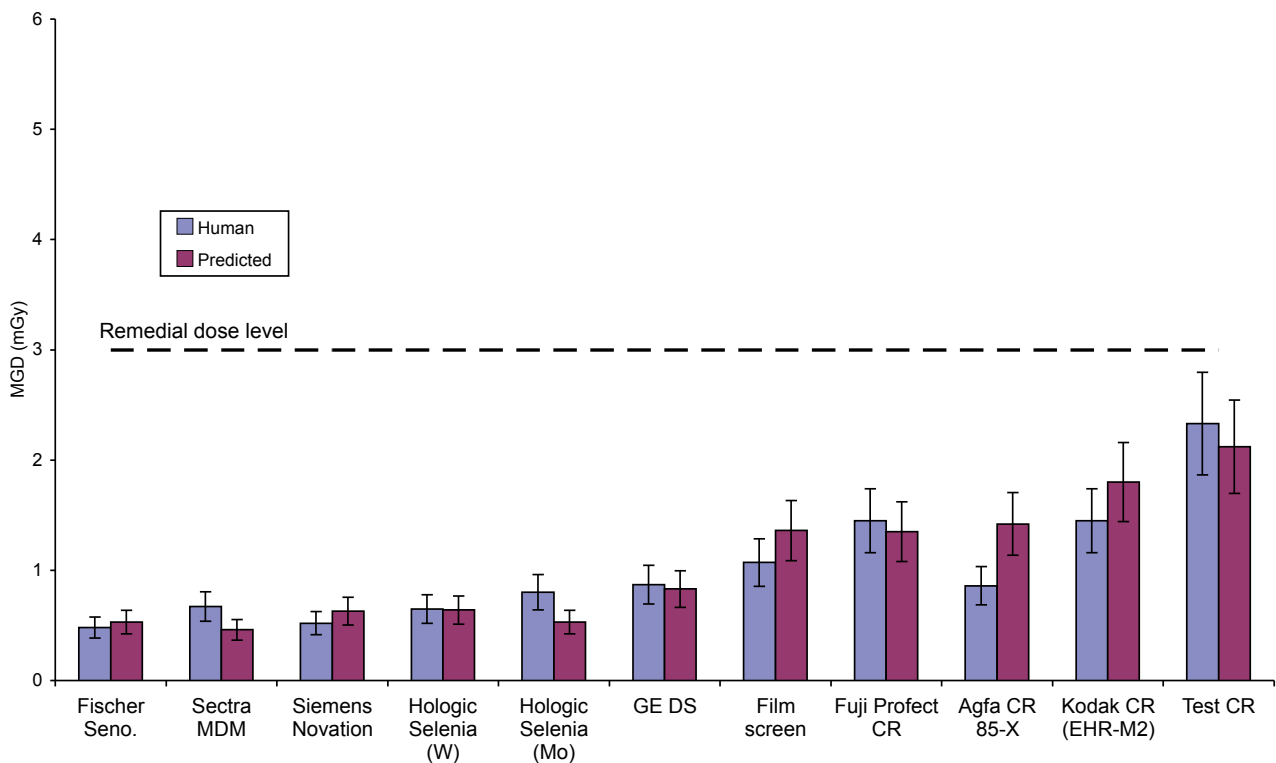


Figure 13 Dose to reach minimum acceptable image quality standard for 0.25 mm detail. Error bars indicate 95% confidence limits.

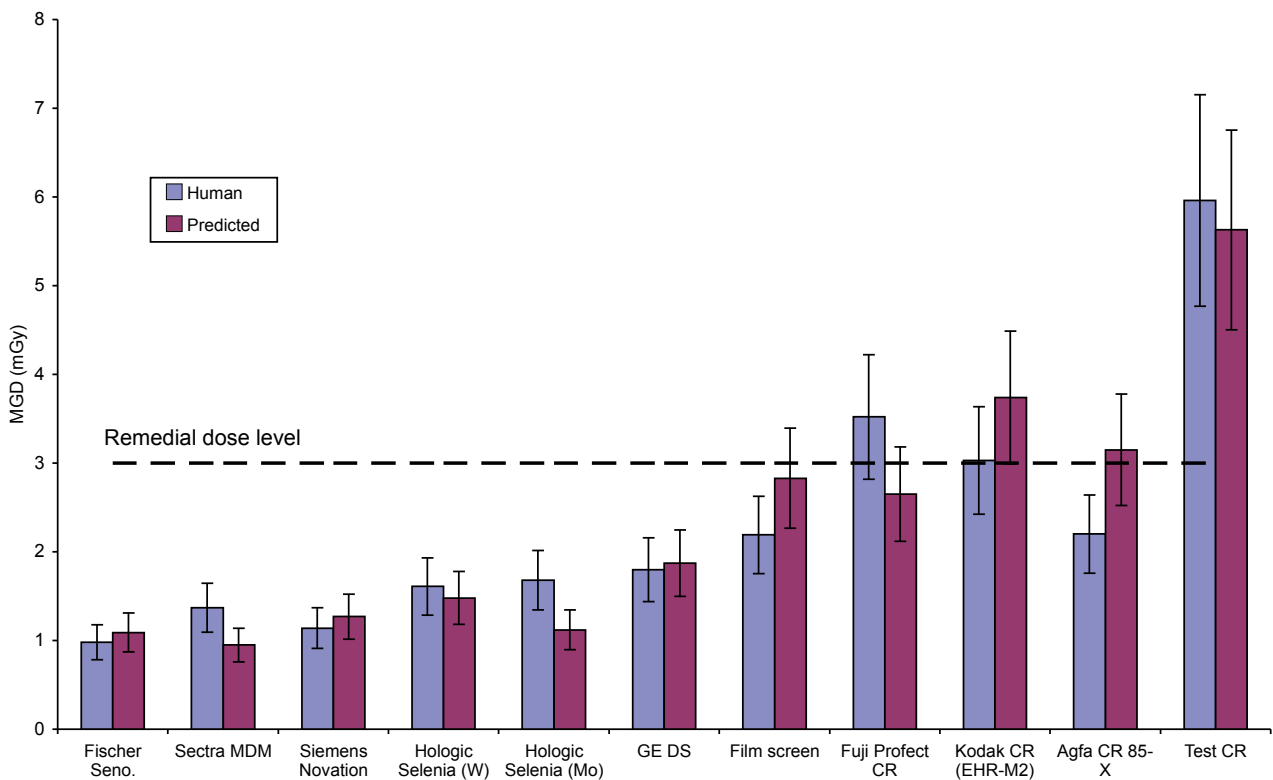


Figure 14 Dose to reach achievable image quality standard for 0.25 mm detail. Error bars indicate 95% confidence limits.

3.6 Optimisation

The target CNR corresponding to the achievable image quality standard was calculated to be 6.0. The MGDs required to reach this target CNR for each beam quality and thicknesses of PMMA are shown in Figure 14. From these data the optimal beam qualities and mAs were calculated and are shown in Table 9. Table 10 shows a similar calculation using the kV/target/filter combinations selected by the AEC in standard dose mode along with the mAs necessary to achieve a CNR of 6.0.

Table 9 Optimal factors to reach achievable image quality (ie where CNR=6.0) at the lowest dose

PMMA thickness (mm)	kV target/filter	BGD pixel value ^a	mAs	MGD (mGy)	Dose compared to standard dose AEC selection	Remedial dose level in NHSBSP protocol (mGy)
20	28 W/Rh	235	41	0.22	37%	1.0
30	28 W/Ag	335	61	0.36	44%	1.5
40	28 W/Ag	371	83	0.62	53%	2.0
45	31 W/Ag	441	113	0.89	60%	2.5
50	28 W/Ag	401	107	1.02	64%	3.0
60	31 W/Ag	511	126	1.60	80%	4.5
70	34 W/Ag	694	133	2.37	95%	6.5

^aBackground pixel values have been offset corrected.

Table 10 Settings required to reach achievable image quality (ie CNR=6.0) using the beam quality selections made by the AEC in standard dose mode

PMMA thickness (mm)	kV target/filter	BGD pixel value ^a	mAs	MGD (mGy)	Dose saving if optimal beam quality used	Remedial dose level in NHSBSP protocol (mGy)
20	25 W/Rh	546	16	0.23	5%	1.0
30	26 W/Rh	542	28	0.37	3%	1.5
40	28 W/Rh	541	45	0.63	1%	2.0
45	28 W/Rh	546	62	0.81	9%	2.5
50	30 W/Rh	514	73	1.09	6%	3.0
60	29 W/Ag	593	100	1.59	0%	4.5
70	32 W/Ag	620	132	2.48	4%	6.5

^aBackground pixel values have been offset corrected.

Technical Evaluation of the Hologic Selenia FFDM System with a Tungsten Tube

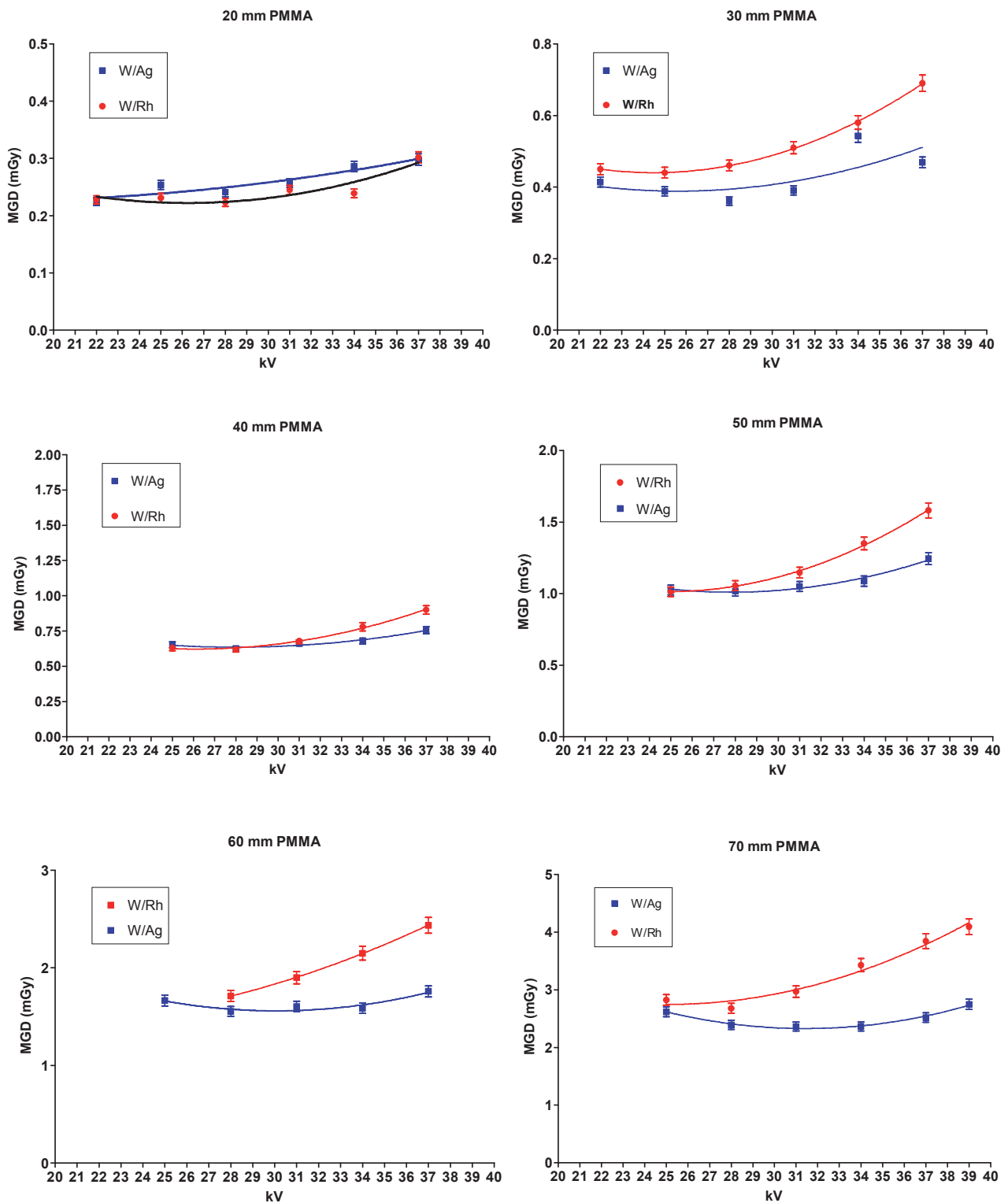


Figure 15 MGD to reach the achievable image quality standard in the NHSBSP protocol (ie CNR =6.0). Error bars indicate 95% confidence limits.

4. DISCUSSION

The detector response was linear with a pixel value offset of about 50. The noise analysis confirmed that quantum noise is the dominant noise source. As with most systems, there was also evidence of some electronic and structural noise. In all three dose modes, the AEC resulted in doses to simulated breasts that were well below the limits in the NHSBSP protocol. The doses for the standard breast simulated with 45 mm of PMMA in the three modes were 1.47, 1.08 and 0.65 mGy. At this thickness, an upper limit of 2.5 mGy is applied by the NHSBSP. The doses displayed by the system were slightly lower than calculated. It is believed that this may be explained by the use of a different breast model to estimate the dose.

The three AEC dose modes resulted in approximately constant background pixel values of about 550, 390 and 210. The AEC chose the W/Rh target/filter combination for simulated breast thicknesses of less than about 70 mm. The W/Ag combination was selected for larger thicknesses. The tube voltage selection rose gradually with increasing thickness. The net result of these choices was that the CNR values were relatively high for thinner breasts but dropped steeply with increasing breast thickness. Comparison with the CNR necessary to reach the achievable and minimum acceptable image quality levels showed that in the standard dose mode the CNR was sufficient to ensure that achievable image quality is met or exceeded at all thicknesses. Using the limited dose mode resulted in CNR values that were much lower but just exceeding the minimum standards in the European protocol.

The image quality measurements indicated that, for the standard thickness tested (equivalent to 50 mm thickness of PMMA, ie 60 mm of typical breast), the image quality was better than the achievable levels at the current standard dose AEC setting. In this mode, the AEC selected a dose of 1.68 mGy using 30 kV W/Rh. This is slightly higher than the 1.58 mGy found when using the AEC in this mode with a 5 cm thickness of PMMA and suggests that the equivalence is not exact or that the AEC was affected by the details in the test object. Figure 9 shows that the use of the low dose mode will result in an image quality between the minimum and achievable. The use of the limited dose mode resulted in a dose of 0.65 mGy, and an image quality close to the minimum standard. A dose of about 0.71 ± 0.15 mGy was calculated to be necessary to reach the minimum image quality level for this equivalent breast thickness. A dose of about 1.48 ± 0.07 mGy was calculated to be necessary to reach the achievable image quality level for this equivalent breast thickness.

A previous report on the Siemens Novation system found that there was a dose saving of about 15% by using a tungsten target with a rhodium filter rather than a molybdenum target with a rhodium filter.¹² In that case all the measurements were on the same system. In this report it is harder to verify the dose advantage of the tungsten target as the comparative measurements are from a different system. The doses required to reach the acceptable and achievable image quality levels are higher than reported previously for the Selenia with a molybdenum tube where automated threshold contrast is used. However, the reverse seems to be true when the thresholds were determined by human readers. It can be expected that the Selenia systems will also show a 15% dose saving by using a tungsten tube. This is consistent with the data shown here, although the errors in the measurements are quite large and it is difficult to confirm this without having the tubes fitted to the same system. It is also noted that all the systems that use the Hologic detector (ie Selenia (Mo), Selenia (W) and Novation) require very low doses to produce excellent image quality.

The optimisation study demonstrated that lower doses were needed where the W/Ag target/filter combination was used with larger breast thicknesses. A tube voltage in the range of 25–28 kV was preferable to the use of higher values with the W/Rh target/filter combination. This finding is similar to that reported in other evaluations in which selenium detectors were used. There was less dependence on kV with the W/Ag target/filter combination. The calculated optimal kV/target/filter combinations shown in Table 8 achieved only modest dose

savings (<10%) compared with the doses shown in Table 9 where the current selections were used. These findings suggest that the current AEC design is close to optimal in terms of beam quality selection. The AEC design allows for three dose levels to be used. The two higher levels clearly pass the requirements of the NHSBSP and European protocols, while the lowest dose level is close to the limit for acceptable image quality.

5. CONCLUSIONS

This system is capable of producing excellent image quality for a relatively low radiation dose. As currently set up, the AEC will be satisfactory for most types of breast in standard and low dose modes. The system met the main standards in the NHSBSP and European protocols. The system should be evaluated clinically by the NHSBSP.

REFERENCES

1. Workman A, Castellano I, Kulama E, Lawinski CP, Marshall N, Young KC. *Commissioning and Routine Testing of Full Field Digital Mammography Systems*. NHS Cancer Screening Programmes, 2006 (NHSBSP Equipment Report 0604) (version 2 available only in PDF format at www.cancerscreening.nhs.uk).
2. Young KC, Johnson B, Bosmans H, Van Engen R. Development of minimum standards for image quality and dose in digital mammography. In *Digital Mammography*, 2005 (IWDM 2004, Proceedings of the Workshop in Durham, NC, USA, June 2004).
3. Van Engen R, Young KC, Bosmans H, Thijssen M. The European protocol for the quality control of the physical and technical aspects of mammography screening. In: *European Guidelines for Breast Cancer Screening*, 4th edn. Luxembourg: European Commission, 2006.
4. Young KC, Cook JJH, Oduko JM. Use of the European protocol to optimise a digital mammography system. In: Astley SM, Bradey M, Rose C, Zwigelaar R (eds). *Proceedings of the 8th International Workshop on Digital Mammography. Lecture Notes in Computer Science*, 2006, 4046: 362–369.
5. Young KC, Oduko JM, Bosmans H, Nijs K, Martinez L. Optimal beam quality selection in digital mammography. *British Journal of Radiology*, 2006, 79: 981–990.
6. Young KC, Cook JJH, Oduko JM, Bosmans H. Comparison of software and human observers in reading images of the CDMAM test object to assess digital mammography systems. *Proceedings of SPIE Medical Imaging*, 2006, 614206: 1–13.
7. Young KC, Cook JJH, Oduko JM. Automated and human determination of threshold contrast for digital mammography systems. In: Astley SM, Bradey M, Rose C, Zwigelaar R (eds). *Proceedings of the 8th International Workshop on Digital Mammography. Lecture Notes in Computer Science*, 2006, 4046: 266–272.
8. Young KC, Oduko JM. *Evaluation of the Kodak DirectView Mammography Computerised Radiography System*. NHS Cancer Screening Programmes, 2005 (NHSBSP Equipment Report 0504) (available only in PDF format at www.cancerscreening.nhs.uk).
9. Young KC, Oduko JM, Woolley L. *Technical Evaluation of the Hologic Selenia Full Field Digital Mammography System*. NHS Cancer Screening Programmes, 2007 (NHSBSP Equipment Report 0701) (available only in PDF format at www.cancerscreening.nhs.uk).
10. Young KC, Oduko JM. *Technical Evaluation of the Kodak DirectView Mammography Computerised Radiography System using EHR-M2 Plates*. NHS Cancer Screening Programmes, 2007 (NHSBSP Equipment Report 0706).
11. Young KC, Oduko JM. *Technical Evaluation of the Agfa CR-85 Mammography System*. NHS Cancer Screening Programmes, 2007 (NHSBSP Equipment Report 0707).
12. Young KC, Oduko JM. *Technical evaluation of the Siemens Novation Full Field Digital Mammography System*. NHS Cancer Screening Programmes, 2007 (NHSBSP Equipment Report 0710).

